AEDC-TDR-63-245

ANALYTICAL AND EXPERIMENTAL STUDIES TO DEVELOP ION ENGINE GROUND-TESTING TECHNIQUES

By

R.A. Hubach

Hughes Research Laboratories

a Division of Hughes Aircraft Company

Malibu, California

TECHNICAL DOCUMENTARY REPORT NO. AEDC-TDR-63-245

November 1963

Program Element 62405184/6950, Task 695003

(Prepared under Contract No. AF 40(600)-948 by Hughes Research Laboratories, a Division of Hughes Aircraft Company, Malibu, California.)

ARNOLD ENGINEERING DEVELOPMENT CENTER

AIR FORCE SYSTEMS COMMAND

UNITED STATES AIR FORCE

NOTICES

Qualified requesters may obtain copies of this report from DDC, Cameron Station, Alexandria, Va. Orders will be expedited if placed through the librarian or other staff member designated to request and receive documents from DDC.

When Government drawings, specifications or other data are used for any purpose other than in connection with a definitely related Government procurement operation, the United States Government thereby incurs no responsibility nor any obligation whatsoever; and the fact that the Government may have formulated, furnished, or in any way supplied the said drawings, specifications, or other data, is not to be regarded by implication or otherwise as in any manner licensing the holder or any other person or corporation, or conveying any rights or permission to manufacture, use, or sell any patented invention that may in any way be related thereto.

ANALYTICAL AND EXPERIMENTAL STUDIES TO DEVELOP ION ENGINE GROUND-TESTING TECHNIQUES

By
R. A. Hubach
Hughes Research Laboratories
a Division of Hughes Aircraft Company
Malibu, California

(The reproducibles used in the reproduction of this report were supplied by the author.)

November 1963

AF - AEDC
Arnold AFS Tenn

ABSTRACT

Techniques for ground-testing of ion engines obtained since publication of AEDC-TDR-62-152 (Sept. 1962) are reviewed. This report discusses procedures for the neutralization of ion beams and the results of experiments measuring the space charge and current neutrality achieved. Results of experiments with the window probe and a new probe for the measurement of beam potential are also presented. Results achieved with the methods described in the first Technical Documentary Report are discussed; more recently developed methods and their results are also reviewed.

PUBLICATION REVIEW

This report has been reviewed and publication is approved.

Eules L. Hively
Acting Chief, Propulsion Division
DCS/Research

Donald R. Eastman, Jr.
DCS/Research

TABLE OF CONTENTS

	ABSTRACT	iii
I.	INTRODUCTION	1
II.	NEUTRALIZATION STUDIES	1
	A. Space Charge Neutralization	1
	B. Current Neutralization	3
III.	MEASUREMENT OF BEAM POTENTIAL	10
	A. Description of Lithium Ion Beam Probe	10
	B. Results of Measurements	13
IV.	MEASUREMENT OF SLOW ION DENSITY	13
V.	AUXILIARY EQUIPMENT	21
VI.	RESULTS AND CONCLUSIONS	21
	ACKNOWLEDGMENT	22
	REFERENCES	35
	APPENDIX – LITHIUM GUN COLLECTOR RESPONSE	37
	LIST OF SYMBOLS	42

I. INTRODUCTION

The first report* (September 1962) published under this contract developed a philosophy for the achievement of the contract objectives; this philosophy has remained unchanged. However, as more information has become available, many of the technical details have been modified. The computer studies have been discarded because of the inherent complexity of the problem, which necessitated the adoption of unrealistic simplifying assumptions. Because of its simplicity, a lithium ion beam probe has been designed, built, and successfully placed in operation as a diagnostic tool and replaces the electron beam probe described previously. Window probe studies revealed the presence of slow ions in the high energy cesium ion beam; their source and their magnitude are being studied. Current neutralization was examined in an isolated engine experiment; it was found that it represents no problem to the operation of ion engines in space.

II. NEUTRALIZATION STUDIES

A. Space Charge Neutralization†

1. Definition and Experimental Techniques

Neutralization is divided into two distinct modes. The first, space charge neutralization, requires equal numbers of ions and electrons within the beam and is not concerned with any charging of the vehicle which might occur. The second, current neutralization, requires the emission of equal numbers of ions and electrons from the vehicle and influences the ultimate potential of the vehicle. Adequate space charge neutralization is necessary for two reasons. First, in extreme cases excessive space charge can actually cause the beam to turn around and return to the vehicle; in this case, no thrust results. Second, in less extreme cases the unbalanced charge will interact with the vehicle and cause a loss of thrust. A slight space charge imbalance may exist, however, without severely limiting engine performance.

In all of the neutralization experiments performed to date (Refs. 1, 2), the ion beam has been pulsed to minimize the interactions of the

*R. A. Hubach and G. B. Peppin. "Analytical and Experimental Studies to Develop Ion Engine Ground-Testing Techniques." AEDC-TDR-62-152, September 1962.

†The work reported in this section was partially supported by Contract NAS 5-517 and is included here for completeness.

beam with its non-space-like environment. The pulse length is kept short compared with the engine-collector spacing, and measurements are generally made near the engine before the beam impinges upon the collector.

To monitor the space charge imbalance in the plasma pulses, two phenomena are utilized which are sensitive to the degree of imbalance existing. The first, which has been monitored only crudely, is the spread of the ion beam when the positive and negative ion densities are not equal. In these experiments measurements have been made only by observation of the ion current which reaches the collector after the electrons have been removed by a grid system. If the beam is unneutralized it expands prodigiously, and very little reaches the collector. If the beam is well neutralized, however, it remains well collimated, and nearly all of it reaches the collector in a properly designed experiment. The second method of detection of a space charge imbalance has been used to gather more refined data and to estimate the degree of neutrality achieved. In this method a conducting hoop surrounds the pulsed beam and charges are induced into it by any uncompensated charges which pass through it. If the charges are in perfect balance, none will be induced in the hoop; when neutralization is imperfect, a pulse of charge resembling a dispersion curve will be exhibited at the hoop. Using these techniques space charge neutralization greater than 99% has been measured.

2. Experimental Comparison of Different Neutralization Schemes

The two main neutralization techniques employed at Hughes can best be described by the terms pre-exit and post-exit neutralization (Fig. 1). These terms refer to the position at which electrons are injected with respect to the exit electrode, the electrode farthest from the emitter. A pre-exit neutralizer usually consists of four button cathodes placed symmetrically around the outside of the beam within the decel region of the engine. In this system a decel voltage ranging from 20 to 200 V must be applied to the electrons to achieve neutralization. The post-exit system is composed of a length of thermionically emitting tantalum wire about 0.010 in. in diameter placed just beyond the exit aperture of the engine. In the post-exit neutralization system no injection voltage has been found to be necessary. The length of the post-exit emitter is apparently not critical; neutralization was achieved with two diametrically opposed filaments, each surrounding only about 30° of the beam, as well as with a single filament almost completely surrounding the beam. Neither emitter was in such a position that it could be struck by ions in the beam.

Results of typical neutralization experiments are shown in Fig. 2 (a), (b), and (c), which correspond to post-exit neutralization, no neutralization, and pre-exit neutralization, respectively. In each case the upper

trace represents the collector current, the middle trace the induced charge on the hoop, and the lower trace the pulse applied to the ionizer. Although there are no significant differences between Figs. 2(a) and 2(c), the lack of collector current and large induced hoop current, which are characteristic of poor neutralization, appear in Fig. 2(b).

From these results it is concluded that space charge neutralization was achieved equally well with both neutralization schemes under the conditions prevailing in this experiment. It is still necessary to verify these results in space and then to choose the method which is more reliable and efficient for use in actual missions. It appears now that the post-exit scheme will be used in the practical applications of surface contact ion engines.

3. Effects of Physical Probes in Beams

The effects on space charge neutralization of probes placed in the beam were examined using the techniques described above. Two metallic probes, one about 0.1 in. in diameter and the second about a tenth that size, were swung through an unneutralized beam. When the larger probe entered the beam the collector current increased appreciably and the hoop trace decreased, indicating that the state of neutralization was strongly influenced by the presence of the probe within the beam. No such effect was observed with the smaller probe.

This experiment indicates that large probes must not be placed in the beam if realistic neutralization data are to be obtained; if their size is kept sufficiently small, however, probes can probably be included without detriment.

B. Current Neutralization

1. Definition and Experimental Techniques

Current neutralization differs from space charge neutralization by integrating any imbalance of current leaving the vehicle; the manifestation of the integrators is an increase in vehicle potential. For this reason a very small imbalance can create very large vehicle potentials which may in turn reduce or eliminate the thrust anticipated from the engine.

To examine this effect the integrating property can be made use of to yield high sensitivity, that is, to obtain a measurable response to only a very small current imbalance. This may be accomplished by isolating the engine and its auxiliary equipment from the ground and allowing it to charge to the voltage dictated by the leakage resistance and current imbalance.

The experimental setup consists of two screen rooms, one completely contained within the other (Fig. 3). The inner screen room is 7 ft high by 6 ft deep by 9 ft long and is separated from the outer screen room by a 1-ft spacing on all sides. All equipment required to power the ion engine and the testing and measuring apparatus is contained within and grounded to the inner screen room. The ion engine, mounted inside a vacuum chamber, is connected electrically to equipment in the inner screen room.

Electrical paths between earth-ground and the inner screen room have been kept at a minimum and appear only as leakage paths through the isolation transformer, the stand-off insulators, and the capacitance between the two screen rooms. The double screen room essentially appears as an RC circuit with the charging current furnished by the charge imbalance in the pulsing ion beam of the engine.

When the ion engine pulse is initiated, the inner screen room will begin to charge for about 50 μsec, the duration of the ion engine pulse. The RC circuit then discharges for 1 msec, the time interval between ion engine pulses. The potential of the inner screen room rises during an ion engine pulse to a maximum potential, discharges to a lower potential, charges to the maximum potential again, and so forth (Fig. 4). Factors controlling the maximum potential are ion engine beam voltage, beam current, pulse length, pulse repetition rate, resistance between ion engine (inner screen room) and ground, and capacitance between ion engine (inner screen room) and ground.

The remaining pages of this section will discuss the relation between the current imbalance (given in percent as 100 times the ratio of the net current leaving the engine to the ion current being emitted) and an easily measurable parameter. This measurement is made by draining a small current through a known fixed resistance R which is small compared with the isolation resistance.

Figure 4 gives the expected voltage versus time variations in engine potential where V_1 and V_o represent maximum and minimum potential, respectively, reached during one charge-discharge cycle; t_d represents the discharge time and t_c the charging time.

The equation describing the engine potential during the discharge period is derived as follows (see Fig. 5(a)):

$$V = i_1 R \quad \text{where } i_1 \text{ is the measured current through the fixed resistance } R$$

$$q = VC$$

$$i_1 = -\frac{dq}{dt} = -C\frac{dV}{dt} = \frac{V}{R}$$

$$\frac{dV}{V} = -\frac{dt}{RC}$$

Integration yields $V = K_1 \exp\left(-\frac{t}{RC}\right)$.

The boundary conditions are

$$V = V_1 \quad \text{when} \quad t = 0$$

and

$$V = V_o \quad \text{when} \quad t = t_d \ .$$

Then $V_1 = K_1$ and

$$V = V_1 \exp\left(-\frac{t}{RC}\right) \tag{1}$$

$$V_o = V_1 \exp\left(-\frac{t_d}{RC}\right) \ . \tag{2}$$

When the ion engine pulse is on, the charging equation is derived as follows (see Fig. 5(b)). Here the net current leaving the ion engine (ion current plus electron current) is represented by i and the leakage current through either a shunt resistance or the isolation resistance of the system by i_2 .

$$V = i_2 R$$

$$q = CV$$

$$i = i_2 + \frac{dq}{dt} = \frac{V}{R} + C\frac{dV}{dt}$$

$$\frac{dV}{\left(i - \frac{V}{R}\right)} = \frac{dt}{C} \ .$$

Integration yields $i - \frac{V}{R} = K_2 \exp\left(-\frac{t}{RC}\right)$.

The boundary conditions are

$$V = V_o \quad \text{when} \quad t = 0$$

and

$$V = V_1 \quad \text{when} \quad t = t_c \ .$$

Therefore, $\left(i - \frac{V_o}{R}\right) = K_2$ and

$$V = R\left[i - \left(i - \frac{V_o}{R}\right) \exp\left(-\frac{t}{RC}\right)\right] \tag{3}$$

$$V_1 = R\left[i - \left(i - \frac{V_o}{R}\right) \exp\left(-\frac{t_c}{RC}\right)\right] \quad . \tag{4}$$

The last of the general expressions we will need before considering the actual values of parameters which are expected to be encountered in the experiment is an expression for $V_1 - V_o$. This is easily obtained in the following form from (2).

$$V_1 - V_o = V_1\left(1 - e^{-\frac{t_d}{RC}}\right) . \tag{5}$$

The following physical parameters are assumed

$$R = 10^8 \Omega$$

$$C \approx 2 \times 10^{-9} \text{ F}$$ (this value was computed from the screen room dimensions; the measured value is slightly less)

$$t_c = 5 \times 10^{-5} \text{ sec}$$

$$t_d = 10^{-3} \text{ sec} \quad .$$

Therefore

$$RC = 0.2 \text{ sec}$$

$$\frac{t_c}{RC} = 2.5 \times 10^{-4}$$

$$\frac{t_d}{RC} = 5 \times 10^{-3} \quad .$$

Several simplifications in computation can be made because

$$1 - e^{-x} \approx x \quad \text{for} \quad x < 0.1$$

Equation (5) becomes, for $t_d/RC = 5 \times 10^{-3}$,

$$(V_1 - V_c) \approx V_1\left(\frac{t_d}{RC}\right) \approx 5 \times 10^{-3} V_1 \quad ,$$

or $\Delta V = 5 \times 10^{-3} V_1$, which is an insignificant variation. Therefore, a constant voltage can be assumed.

If R_s is chosen at $10^7 \Omega$, then $t_d/RC = 0.05$; the expansion approximation still holds and $V_1 - V_o = 0.05\ V_1$, a tolerable 5 % variation. This indicates that if the experiment is to be conducted with straightforward simplicity, the effective shunt or leakage resistance must not be less than $10^7 \Omega$, an achievable value.

As stated previously, the quantity desired is the net current i from the ion engine through the isolation system. By charge conservation it is clear that in the equilibrium state the leakage current is given by the net current times the ratio of the charging time to the period of one cycle.

$$i_2 = \frac{t_c}{t_d + t_c}\ i \approx 0.05\ i \quad .$$

It has been shown that i, the net current, approximately equals a constant times the measured leakage current, i.e., the average steady-state engine potential divided by the total system-to-ground resistance. Hence, the net current can be translated easily and directly from the ammeter reading of the leakage current.

2. Experimental Results

The stray capacitance was calculated to be 2×10^{-9} F and was measured in the fully instrumented screen room without an ion engine to be 1.5×10^{-9} F. The leakage resistance of the entire system complete with an unheated ion engine was greater than $10^9 \Omega$. It was decided that the fixed resistance should be an order of magnitude less than the leakage resistance; thus it was set at $10^8 \Omega$. Most of the current now flows through the fixed resistor, and measurement yields accurate knowledge of the screen room potential. In the cw case an ammeter in series with the fixed resistor is sufficient to measure the screen room potential; in pulsed experiments an oscilloscope replaces the ammeter to record the transient response. Results of the cw and pulsed experiments are discussed below.

a. The CW Experiments — The cw experiments with the isolated engine designed to test current neutrality are more meaningful than cw space charge neutrality experiments. In space charge neutralization a single electron can contribute to the neutralization of several ions merely by remaining in the vicinity of the ion beam for a long period of time. Therefore, the yield of electrons created by gas ionization or secondary emission from bombarded surfaces can be quite small and space charge neutrality can still be achieved if the electrons linger in the ion beam. Requirements for current neutrality in the cw ion beam differ completely. If the engine is isolated from its surroundings, each ion that leaves the engine must be either accompanied by an electron or replaced by another ion. When this condition is not fulfilled the engine will charge to the beam acceleration potential or to whatever potential is dictated by the current imbalance and degree of isolation achieved.

Post-exit neutralization implemented by means of a 7-mil tantalum wire heated to emit electrons thermionically was used; pre-exit neutralization was not attempted. The electron emitter is stretched around the entire periphery of the ion beam in such a position that it is not struck by the ions as they pass. A voltage V_E may be placed between the exit electrode and the electron emitter, which is heated by a dc voltage of about 20 V (see Fig. 6).

The results of the cw experiments are shown in Fig. 7, where the parameter is the neutralizer-exit voltage V_E . In all cases the engine and screen room charged to the potential applied to the beam until electrons were made available by the electron emitter. It was possible to set the potential to nearly any desired value (within the limits shown in Fig. 7) by varying the temperature of the electron emitter. In certain regions, however, the engine potential was very sensitive to small changes in emitter temperature; therefore it was difficult in practice to obtain particular voltages between about -16 V and beam potential. This is not unexpected since the electron emission is very strongly dependent on the thermionic emitter temperature. For voltages more positive than about -16 V , however, a great many more electrons are apparently required and a change in V_N of 1 or 2 V is necessary to make the screen room and engine appreciably positive.

It is extremely important that the screen room and engine could be driven positive at all by the emission of electrons; this removes the limitations which might otherwise have been placed on the sensitivity of the experiment. It was thought that if the engine remained a few volts negative it might draw slow ions from the plasma and contribute to the neutrality. When the engine reaches 0 V it does not seem likely that this will happen and it appears even less likely at +66 volts, the most positive voltage reached in this experiment. At 0 V the leakage current must also be zero; at positive voltages the leakage current does not limit the sensitivity of the experiment. Notice in Fig. 7, however, that a positive potential

was not reached when the neutralizer was positive with respect to the exit electrode. The limitations mentioned above do apply in this case, and more extensive experimentation on these effects is required.

On the basis of these and the space charge neutrality experiments performed previously, it seems absolutely safe to state that the vehicle can be maintained with a negligible amount of excess charge and that there need be only a minute loss of thrust, if any, from a space charge imbalance in the beam. These remarks only apply to post-exit neutralization, since the isolation experiment has not been performed with a pre-exit neutralizer.

To the best of our knowledge this is the first time current neutralization has been demonstrated in such a straightforward experiment. The results appear unambiguous and allow us to contemplate the forthcoming space tests with confidence.

b. The Pulsed Experiments — The pulsed experiments are as yet perhaps less definitive than the cw ones, but they indicate the same ease of neutralization and at least one other significant result. It can be seen that electrons emitted from electrodes within the engine, particularly the accel electrode, can contribute appreciably to current neutralization. To demonstrate the results of the pulsed current neutralization experiments a series of photographs of the scope traces of screen room potential versus time are shown in Fig. 8. At the initiation of each trace a sharp induced pulse corresponds to the pulse applied to the ionizer.

Figure 8(a) shows a typical trace corresponding to an unneutralized ion beam. In amplitude this potential does not reach the beam potential but is limited by the pulse length, current flow, and capacitance of the system. For this particular trace if the amplitude is taken to be -650 V and the capacitance 1.5×10^{-9} F, the average current during a pulse can be calculated to be 24.4 mA. This figure is only approximate, however, since the capacitance is not accurately known and no check was possible because the collector assembly was not completed. In Fig. 8(b) the conditions are identical to those of Fig. 8(a) except electrons are injected at the post-exit emitter. It is not possible to determine the voltage level exactly, as in the cw case, but it is certainly very low and neutralization must be nearly complete.

A current of about 37 mA must be responsible for the amplitude of the unneutralized screen room pulse in Fig. 8(c) in which the ionizer voltage pulse height has been increased to 8 kV. The trace in Fig. 8(d) was recorded under identical conditions but with -300 V on the accel electrode. Current neutralization is nearly achieved when the accel electrode potential is added, apparently because electrons may now be

ejected from the engine by fields which exist within it. These electrons seem to be emitted thermionically from the hot cesium-coated accel electrode.

In some cases the number of electrons emitted is insufficient to cause current neutralization but will appreciably increase the rate of decay of engine potential. Insufficient electrons are injected by the neutralizer in Fig. 8(e), and the decay time is about a factor of five shorter than that in Fig. 8(c), although the amplitude of the engine potential pulse is very nearly the same. This same effect can be observed in Fig. 8(f), (g), and (h) where thermionic electrons from the accel electrode are being emitted. In Fig. 8(f) the cesium boiler valve is open and the accel electrode probably coated with cesium, causing enhanced electron emission and rapid decay of the engine potential. In Fig. 8(g) and (h) the valve has been closed for 5 and 10 min, respectively, and the decay time has increased appreciably in each instance as cleaning up of cesium from the accel electrode proceeds.

As the pulse length is increased, a longer charge time is provided and the maximum potential reached by the screen room will increase almost in direct proportion. This is shown in Fig. 8(i) and (j), where all parameters are identical except the pulse lengths, which are 40 and 20 μsec, respectively. The amplitude of the screen room potential in the case of the 40-μsec pulse is nearly double that of the 20-μsec pulse, as was anticipated. (Pertinent parameters for Fig. 8 are seen in Table I.)

III. MEASUREMENT OF BEAM POTENTIAL

A. Description of the Lithium Ion Beam Probe

In the first Technical Note a method of measuring beam potential was described which involved the use of an electron beam modulated at microwave frequency and the measurement of the phase shift produced as the region of unknown potential was traversed. By the use of high frequency modulation such a probe would potentially yield excellent time and spatial resolution; its development, however, turned out to be a rather major undertaking. The same information may be obtained from a beam of lithium ions (Ref. 3) but some resolution is sacrificed.

Operation of the lithium ion beam probe is extremely simple in principle. Lithium ions are ejected from a gun with an energy (in volts) of V_B and traverse a potential distribution within the cesium

TABLE I

Pertinent Parameters for Current Neutralization Experiments

Figure Number	Pulse Width, μsec	Time Between Pulses, msec	Pulse Height, kV	Voltage on Accel Electrode, V	Time Scale, μsec cm	Voltage Scale Ordinate of Scope Trace, V cm	Cesium Boiler Valve Condition	Neutralizer Condition	Demonstrates
8(a)	40	9	6.0	0	200	500	Open	Off	Unneutralized ion beam - 6 kV
8(b)	40	9	6.0	0	200	500	Open	On	Neutralized ion beam - 6 kV
8(c)	40	9	8.0	0	1000	500	Closed	Off	Unneutralized ion beam - 8 kV
8(d)	40	9	8.0	300	1000	500	Closed	Off	Shows neutralization by electrons from the accel electrode
8(e)	40	9	8.0	0	1000	500	Closed	Partially on	Shows decrease in decay time caused by injected electrons
8(f)	40	9	8.0	0	1000	500	Open	Off	Short decay time with valve open
8(g)	40	9	8.0	0	1000	500	Closed for 5 min	Off	Longer decay time with valve closed
8(h)	40	9	8.0	0	1000	500	Closed for 10 min	Off	Still longer decay time with valve closed for longer period
8(i)	40	9	4.0	0	1000	100	Closed	Off	Effect of pulse width on amplitude of screen room potential
8(j)	20	9	4.0	0	1000	100	Closed	Off	

ion beam where they encounter some maximum positive potential V_M. The value of V_M encountered depends upon many factors — cesium ion density and energy, degree of neutrality, background pressure, and other properties of the environment. Differing values of V_M will also be met, depending on where on the cross section of the cesium beam the lithium ions make their traversal. Consider the variation of the current to the lithium collector (which collects ions after their traversal of the cesium beam) as V_B is increased from zero. At first the lithium collector current is zero since the ions have insufficient energy to overcome the potential barrier encountered, the peak of which is V_M. In fact no current reaches the lithium collector until V_B equals the particular value of V_M encountered. At this time there is a sharp increase to the value of collector current experienced when there was no cesium beam present. The value of V_B recorded at the time of the sudden increase in lithium collector current is equal to the value of V_M encountered by the lithium ions. A schematic diagram of the experimental setup is shown in Fig. 9(a).

To insure that the lithium ions do not appreciably alter the potential they are supposed to be monitoring, their density is kept considerably below that of the cesium ion beam. For the data shown in Fig. 10 the density difference was over four orders of magnitude.

Figure 9(b) shows a cross section of a hypothetical potential which might exist within the cesium ion beam; the cross section passes through the center line of the beam. Let the boundaries of the lithium beam traversing this potential distribution and traveling into the plane of the paper be defined by points A and B. Since the cesium beam is assumed to have cylindrical symmetry, the curve of Fig. 10(a) represents the maximum potential encountered by any portion of the lithium beam. Clearly the maximum potential encountered by the lithium ions on boundary A is different from that encountered by those on boundary B. Such a variation in maximum potential observed across the width of the lithium beam will cause a gradual rise in collector current with increasing lithium ion energy, as was observed in the data of Curve II on Fig. 10. The difference in maximum potential encountered across the lithium beam can be decreased by moving points A and B closer together, which may be accomplished by decreasing the size of the lithium beam collected.

Even if the size of the beam could be made infinitesimal, there would still be a finite slope of the collector current versus beam energy curve. In this case the slope would be caused by variations in energy of the lithium ions within the beam and temporal fluctuations in the potential within the cesium beam.

A great advantage in the use of the lithium beam probe over the electron beam probe resides in its ability to measure unambiguously the potential variation across the cesium beam. This is accomplished by mechanically moving the lithium beam in the direction normal to both beams and monitoring the beam potential at regular intervals. This is represented by moving points A and B along the abscissa in Fig. 9(b); the potential distribution monitored is exactly that represented by Fig. 9(b). Measurements to date have been made only at random points on the cesium beam, and there has been no attempt to record the potential distribution.

B. Results of Potential Measurements

Preliminary experiments have been performed with the lithium beam probe, both with and without a cesium ion beam. The results are encouraging but are not exactly as anticipated, since it was expected that without a cesium beam the lithium collector current would increase with V_B to some saturation value and remain nearly constant at that level. This did not occur and one or more peaks were observed (Fig. 10) at reasonably low voltages. We believe that this anomaly is caused by the beam focusing effects of V_B, and the analysis of the Appendix shows that this is probably the case.

Curve II of Fig. 10 was obtained under exactly the same circumstances as Curve I, except that the cesium beam was intervening between the lithium source and the collector. Notice that the current increase occurred over a range of about 20 V, indicating that the maximum potential encountered across the beam of collected lithium ions varied by this amount. During this particular run the collimating aperture was 1/2 in. in diameter, but it has since been reduced by a factor of four to increase the sensitivity (as discussed in Section III-A).

The results of the measurements taken to date indicate that the maximum beam potential is close to 100 V at a background pressure of about 10^{-5} mm Hg.

IV. MEASUREMENT OF SLOW ION DENSITY

In order to observe slow ions created in the beam by charge-exchange or gas ionization, the window probe (Ref. 4) was biased negatively. While searching for slow positive ions, the window was directed away from the high energy cesium ions. Interpretation of the results is extremely difficult, however, because of the complex characteristics

(even under the most ideal conditions) of Langmuir type probes and because of the decided lack of ideal conditions for these experiments. Specifically, it is assumed that the slow ions result from gas ionization, but the fact that they have undergone an ionizing collision implies that their previous Maxwellian energy distribution has been seriously altered. Thus, an adequate analysis of the window probe data would have to begin with the assumption that the gas possesses a Maxwellian distribution. We must then take account of the modifications to this distribution by the ionizing collision, and, finally, we must determine the response of the probe to the modified velocity spectrum.

Fortunately, this analysis need not be performed in its entirety for useful information to be gleaned from the experimental observations. For instance, it is not unreasonable to assume that the residual gas possesses a Maxwellian distribution prior to its disturbance by the ion beam and that the net effect of the ionizing interactions is to superpose a drift velocity on the newly ionized particles in the direction of travel of the cesium beam. There will also be newly acquired transverse components, but they would not enhance the window probe current. For this reason the calculations of slow ion density from window probe measurements based on a Maxwellian distribution of velocities will always be smaller than the true density. It may be possible to estimate the extent of the velocity changes which occur during the ionizing interactions to obtain a better estimate of the actual slow ion density, but this has not yet been attempted.

It has not been proven conclusively that the slow positive ions are created by gas ionization, although it is difficult to explain their existence by any other means. To firmly establish the source of the slow ions, an experiment must be performed in which different gases are used in the vacuum chamber and the variation of the positive ion densities studied as a function of pressure. Because of the varying masses and ionization cross sections, the response of the probe should vary appreciably with different gases. In particular, a factor of more then 10 exists (Table II) between the expected responses of helium and xenon.

One striking aspect of these data, which has also appeared previously in data taken with the larger annular ion sources, is the existence of a fairly well-defined density level above which there are only small changes in the window current (Fig. 11). From the preliminary experiments, this critical point appears not to be a function of the gas present in the chamber, but to be dependent on the size of the chamber in which the experiments are being performed. Moreover, in the two sets of data which have shown this critical density, it corresponds approximately to the point at which the mean free path of the ions becomes equal to the distance between the engine and collector The two sets of data were taken in different chambers where the engine-collector spacing, and hence the critical density, varied by about a factor of three.

TABLE II

Predicted Values of Probe Current for Various Gases

ELEMENT	$M^{1/2}$[a] (atomic weight)	σ_I[a] at 500 V (Ref. 5) (cross section)	$M^{-1/2}\ \sigma_I^{0.8}$ (Ref. 3) (probe current)
Helium	0.45	0.1	0.36
Neon	1.00	1.00	1.00
Argon	1.40	5.0	2.6
Krypton	2.02	7.0	2.3
Xenon	2.54	22.0	4.7

[a]Relative to neon at 1.00

While it is impossible to draw firm conclusions from such data, the implication is clear that there is a significant contribution to the probe current from portions of the beam up to one mean free path from the probe, and that as the mean free path becomes less than the engine-collector distance, the attenuation of the slow ion flux by scattering roughly compensates for the increase in current caused by the increased gas density. Many more experiments will be necessary, however, before this hypothesis will be confirmed or denied.

In the region surrounding an annular ion beam there appear to be two distinct regions of slow positive ions, one of which shows a definite pressure dependence. The pressure dependent portion occurs within the hollow of the annular beam where the beam does not actually strike the probe. The pressure independent portion is that which actually lies within the beam of cesium ions and may be caused by a phenomenon other than slow ions. In order to calculate the density of slow ions from the current measured by the window probe it is necessary to make several assumptions. The equation employed in these studies, (eq.(6)), is one derived by Schulz and Brown (Ref. 6) in which grossly simplifying assumptions are made. It is used because the data obtained in these preliminary studies probably do not merit a more sophisticated treatment, and accuracy better than a factor of two would be fortuitous.

$$n_B = \frac{I_w}{A_w e} \left(\frac{kT_-}{\epsilon M} \right)^{-1/2} \tag{6}$$

where

I_w ≡ window current

A_w ≡ area of window

e ≡ electronic charge

ϵ ≡ base of natural logarithms

T_- ≡ electron temperature (taken to be 12,000°K)

k ≡ Boltzmann constant

M ≡ mass of positive ion

We will first consider the pressure independent part which appears at the two positions where the high energy ions actually strike the probe as it is swept through the beam (Fig. 12). Since there is no pressure dependence, it is unlikely that these slow ions are created by interaction of the cesium ions with the residual gas. A possible explanation is that the charge-exchange process creates slow positive ions which might be collected

at the window of the probe. In this process a high energy cesium ion interacts with a neutral cesium atom which was emitted unionized from the hot tungsten surface, removing an electron from the atom to replace the ion's missing electron.

After the interaction there remains a slow cesium ion and a high energy cesium atom; the slow ions will certainly contribute to the background plasma if they are sufficiently abundant. The cross section for this process is reasonably well known (Ref. 7) and from the measured window currents it is possible to calculate the density of neutrals necessary to create the observed plasma. Such a calculation is not extremely accurate because of simplifying assumptions which must be made concerning the energy distribution of the slow ions. Values of the neutral cesium density necessary to produce the observed plasma density are calculated from (7), below, and a typical result corresponding to the data of Fig. 12 yields a neutral particle density of about $5 \times 10^{11}/cm^3$. This is much higher than the neutral density anticipated, making charge exchange an unlikely contributor to the observed currents.

$$n_o = \frac{v}{L}\left(\frac{J}{e}\,\sigma_{EX}\right)^{-1} n_B \tag{7}$$

where

n_o ≡ neutral cesium density

n_B ≡ random plasma density

v ≡ velocity of slow ions (taken to correspond to a Maxwellian temperature of 1500°K)

L ≡ a characteristic dimension of the ion beam (2 cm)

J ≡ high energy cesium ion current density

σ_{EX} ≡ cross section for charge exchange.

Some typical data, presented in Table III, show the random plasma density n_B varying with beam density; this was to be expected for any reasonable process. In all cases, however, the neutral particle density would have to be extremely high to account for the presence of such a

dense plasma of slow ions. It appears that, for the time being, the presence of the pressure independent portion of the plasma must remain without adequate explanation.

TABLE III

Dependence of Slow Ion Density on Cesium Ion Beam Density

Density of High Energy (1.2 kV) Ion Beam, $1/cm^3$	Density of Slow Ions n_B, $1/cm^3$
3.3×10^8	1.4×10^8
1.3×10^8	0.6×10^8
0.7×10^8	0.2×10^8

The portion of the plasma inside the annulus shows a distinct pressure dependence which probably results from gas ionization. To check this hypothesis it is necessary to calculate the cross section for gas ionization of air by cesium ions and to compare the value deduced with values ascertained by other methods. The cross section for gas ionization is calculated from

$$\sigma_I = \frac{en_B}{N_o J \tau_1}$$

where N_o is the density of particles in the residual gas, and τ_1 is the length of time a newly created gas ion lingers in the vicinity of the ion beam. To establish τ_1, a characteristic dimension of the ion beam (8 cm) is divided by the velocity of a 300°K air molecule. The results of such calculations based on the data of Fig. 12 are presented in Table IV. Remarkable consistency of the calculated values of σ_I results when the possible large errors in nearly all the quantities used in the calculations are considered. From these data a value of σ_I equal to $4 \times 10^{-17} cm^2$ might reasonably be adopted for comparison with previously determined

values of σ_I. This result is presented in Fig. 13 and is certainly not in contradition to the anticipated result. On the basis of these data it seems safe to conclude that the pressure dependent part of the slow ion plasma is the result of ionization of the residual gas.

TABLE IV

Calculation of σ_I from Plasma Density Measurements

Cesium Beam Voltage = 1.2 kV

Data from Fig. 2 Curve	N_o, $1/cm^3$	τ_1, sec	J, A/cm^2	n_B, $1/cm^3$	σ_I, cm^2
a	3.5×10^{11}	1.7×10^{-4}	1.2×10^{-4}	3.6×10^{6}	8.2×10^{-17}
b	1.7×10^{12}	1.7×10^{-4}	1.2×10^{-4}	7.2×10^{6}	3.4×10^{-17}
c	3.5×10^{12}	1.7×10^{-4}	1.1×10^{-4}	7.2×10^{6}	1.8×10^{-17}
d	9.8×10^{12}	1.7×10^{-4}	1.15×10^{-4}	2.6×10^{7}	2.2×10^{-17}

Regardless of the cause of the slow ion plasma, it presence is obviously of great importance to simulation considerations. The existence of a plasma of density comparable to that of the ion beam will drastically alter the potential distribution across the beam and will therefore affect the distribution of electrons responsible for the neutralization of the ion beam. Although the level of slow ion density which can be tolerated while still maintaining an adequate state of simulation has not been demonstrated analytically, it would seem safe to operate with the slow ion density at less than 1 % of the beam density. Based on this criterion and on the data presented here, it appears that the pressure must be maintained below 5×10^{-6} mm Hg to assure a sufficiently low level of slow ion density.

It is also possible to obtain the cross section for the interaction which liberates electrons to neutralize the ion beam by measuring the fill-up time — the length of time required for a completely unneutralized beam to become neutralized by these spurious electrons. The cross

section obtained in this manner will be greater than the actual gas ionization cross section for two reasons. First, it is difficult to be sure that all the electrons have been removed from the ion beam, and second, other sources such as interactions with the vacuum chamber walls and collector may contribute electrons. The cross section for gas ionization by cesium ions of argon and neon has been investigated (Refs. 5, 8) and the values obtained are shown in Fig. 13. While these curves are not directly applicable to the interaction being investigated because the residual gas had approximately the composition of air, it might be expected that the corresponding curve for cesium ions in air would be between those for neon and argon since the molecular weight of air lies roughly halfway between neon and argon.

If we represent the fill-up time by τ_f, the density of the residual gas by N_o, and the velocity of the cesium ions by v, then the cross section for production of the neutralizing electrons is given by (Ref. 9)

$$\sigma_I = \frac{1}{N_o \tau_f v}$$

Table V gives values of σ_I calculated for N_o varying by more than an order of magnitude. The values of τ_f in Table V were taken from the data displayed in Fig. 14. It is encouraging that the σ_I's thus tabulated show such remarkable consistency despite the possibility of appreciable errors in both N_o and τ_f. These results would lead to the adoption of a value of 1.5×10^{-16} cm^2 for σ_I at 4.0 kV, about a factor of two higher than anticipated. The consistency of the results, however, is encouraging and the high values obtained for σ_I are not inconsistent for the reasons already noted.

TABLE V

Cross Section for Liberation of Neutralizing Electrons

Calculated from Fill-up Time Measurements

N_o, 1/cm^3	τ, sec	v, cm/sec	σ_I, cm^2
1.4×10^{11}	4×10^{-3}	7.6×10^6 (4 kV)	2.3×10^{-16}
4.6×10^{11}	2×10^{-3}	7.6×10^6	1.5×10^{-16}
1.8×10^{12}	5×10^{-4}	7.6×10^6	1.5×10^{-16}
3.5×10^{12}	3×10^{-4}	7.6×10^6	1.3×10^{-16}

V. AUXILIARY EQUIPMENT

In the performance of these experiments certain items are taken for granted which have been developed under this contract with considerable effort. The source of ions used in many of these experiments is a cesium contact button engine capable of current densities up to 15 mA/cm^2 at about 10 kV total accelerating voltage. This source has proven to be quite reliable and has been through several temperature cycles and operated satisfactorily for many hours.

For the support and movement of probes under vacuum, a probe stand which can reproducibly position a probe within 0.005 in. is in operation in the 5-ft diameter vacuum chamber. With this device probes can be moved about 16 in. in either the transverse or longitudinal direction and can be rotated through 360°.

VI. RESULTS AND CONCLUSIONS

Many of the experiments being performed under this contract are in the preliminary state and will be reported more fully in later reports. The results gathered to date are listed below and those that are preliminary are indicated as such.

1. Laboratory experiments have been performed on space charge neutralization which indicate that there is nothing to distinguish pre- and post-exit neutralization.

2. The experiment designed to study current neutralization has been performed and it has been demonstrated as conclusively as possible in the laboratory that this factor will not present an obstacle to the successful operation of an ion engine in space.

3. Preliminary measurements of the cesium ion beam potential have been made.

4. The density of slow ions presumably created by gas ionization has been measured and it has been concluded that they do not create a problem as long as the pressure is maintained at less than 5×10^{-6} mm Hg. This result will be investigated further in the beam potential experiments.

5. A button ion source and extremely accurate probe stand have been constructed and are in operation.

ACKNOWLEDGMENT

The author would like to acknowledge the significant contributions of J. W. Ward, N. B. Kramer, J. A. Kelley, F. I. Krausse, and H. R. Friedrich to the work reported herein.

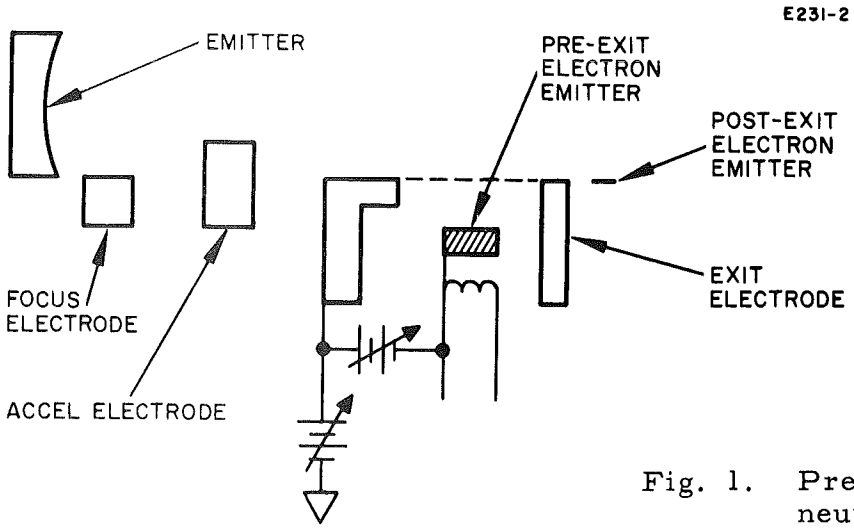

Fig. 1. Pre- and post-exit neutralization schemes.

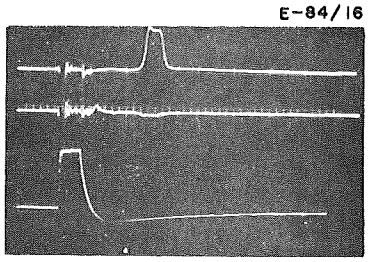

(a) POST-EXIT NEUTRALIZATION
ALTERNATIVE NEUTRALIZER

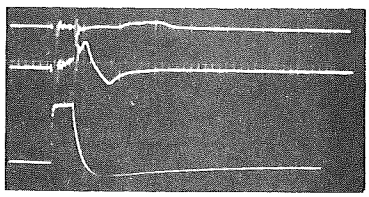

(b) NO NEUTRALIZATION

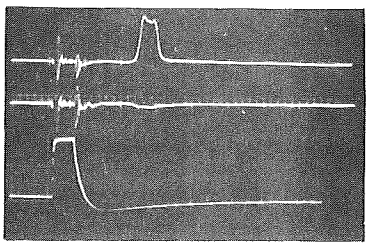

(c) PRE-EXIT NEUTRALIZATION
TRAP NEUTRALIZER

Fig. 2.

Comparison of pre-exit and post-exit neutralization. Upper trace is collector current, scale = 1 mA/div; middle trace is induced hoop current, scale = 0.5 mA/div; time scale = 10 μsec/dib. Neutralization is indicated in (a) and (c) by the presence of collector current and by the lack of induced hoop current. Lower trace is pulse applied to ionizer, scale = 1 kV/div.

M 2542

Fig. 3. Screen room.

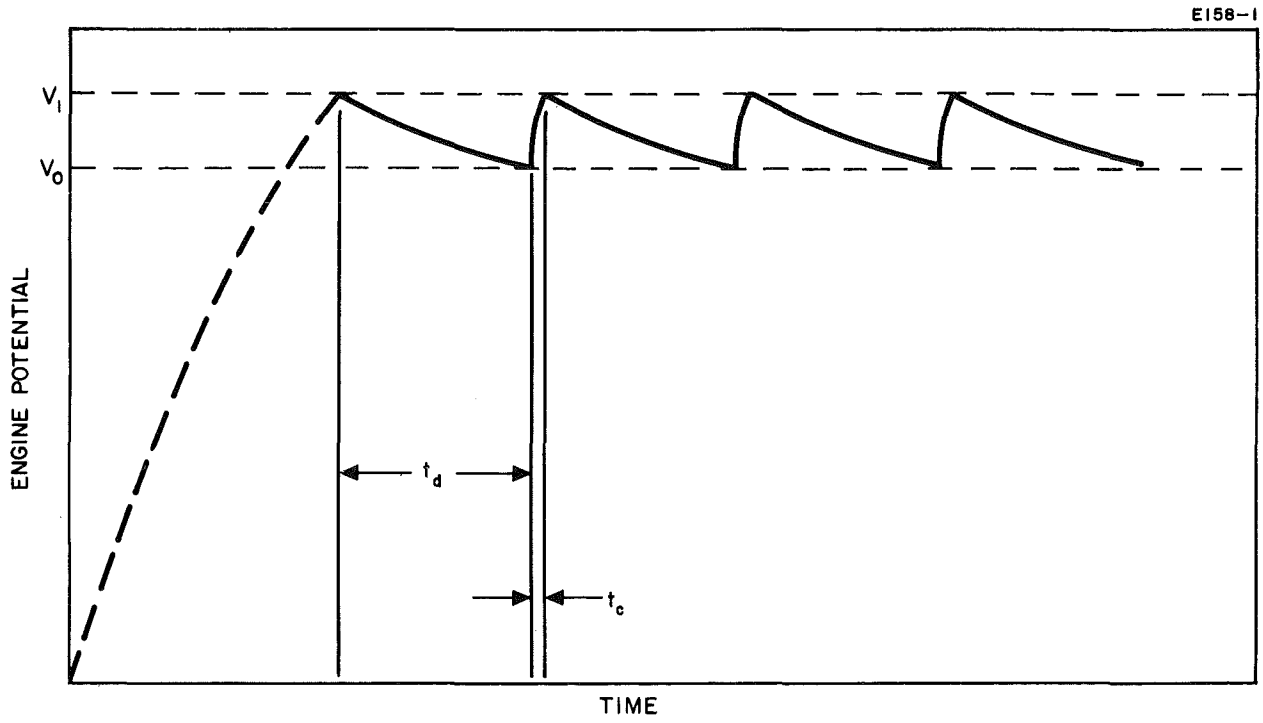

Fig. 4. Variation of potential on the isolated engine during several charge-discharge cycles.

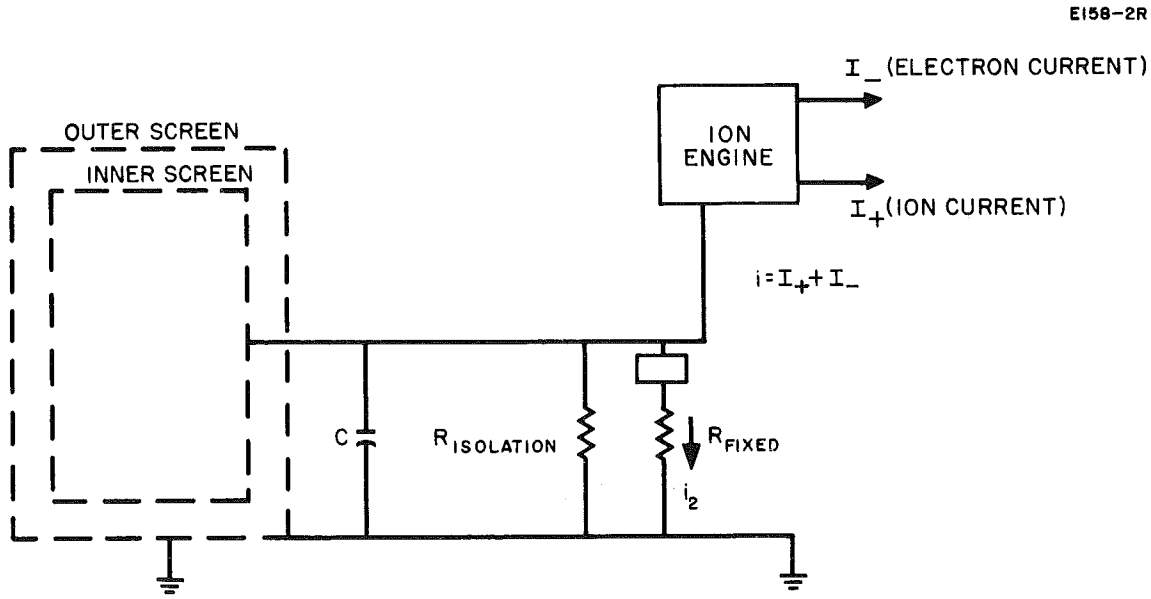

(a). charging conditions

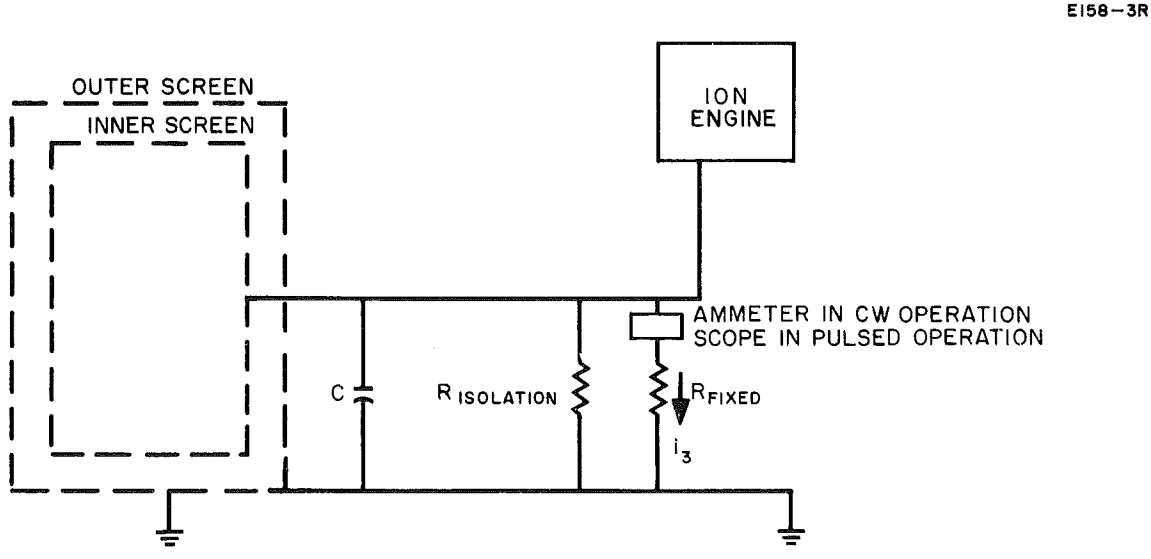

(b). discharging conditions

Fig. 5. Charging and discharging conditions in the engine isolation experimental setup ($R_{fixed} << R_{isolation}$).

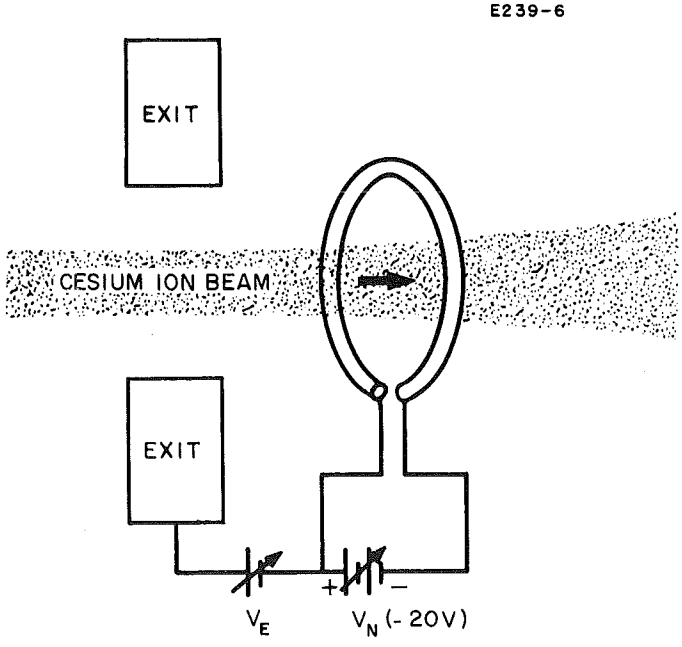

Fig. 6. Schematic of post-exit neutralization scheme.

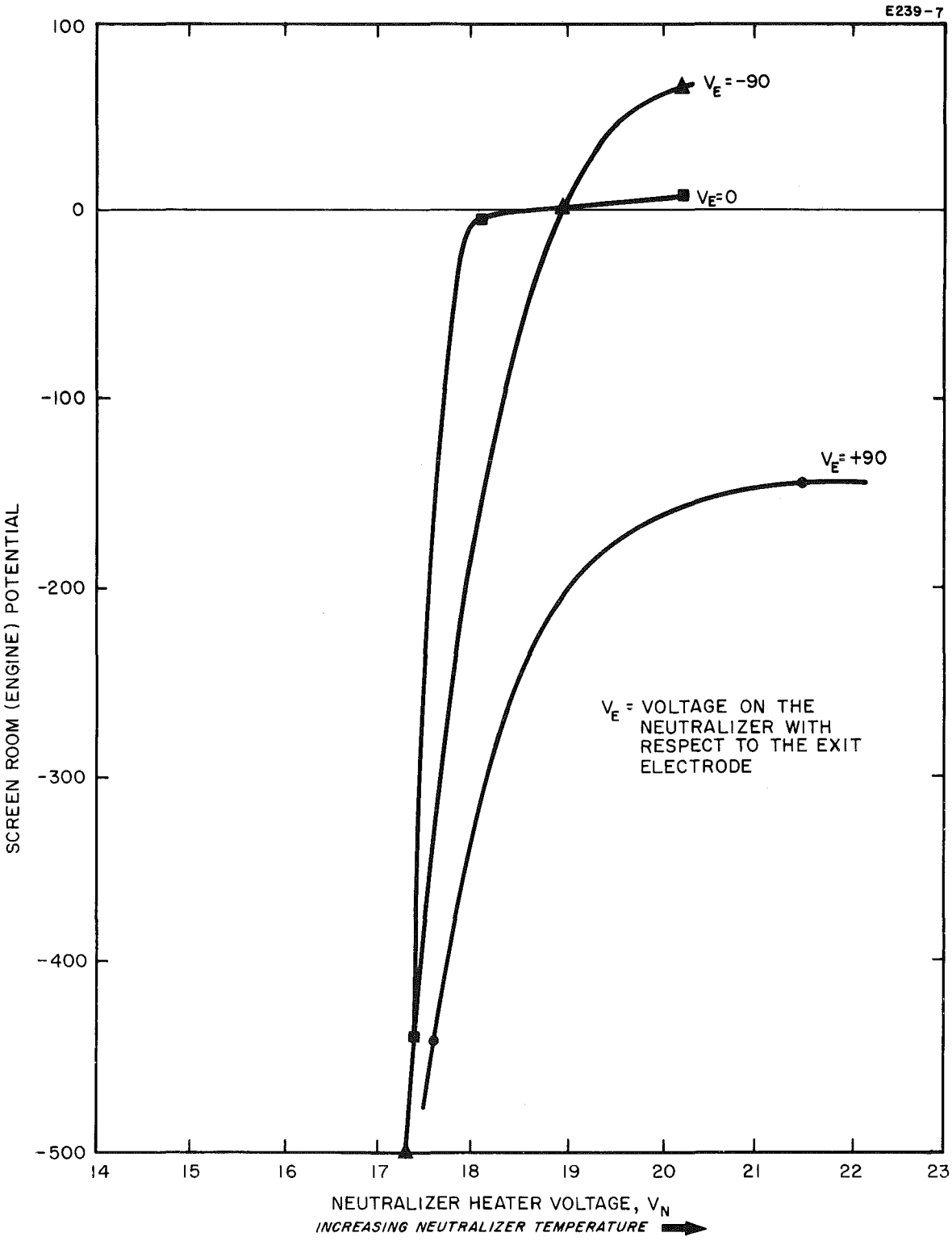

Fig. 7. Screen room potential as a function of neutralizer temperature. At V_n less than 17 V, the screen room potential rose rapidly to ionizer potential, - 3.2 kV.

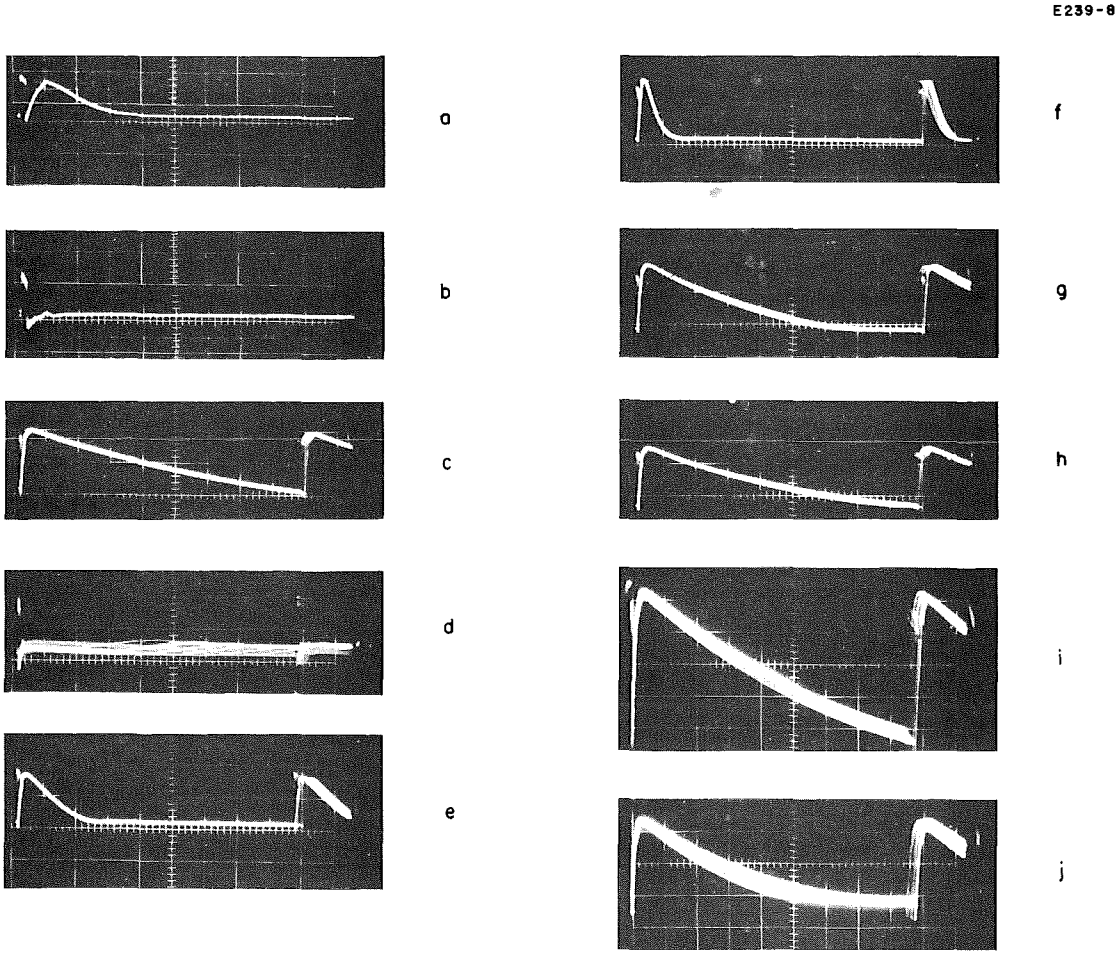

Fig. 8. Traces of screen room voltage versus time after pulse. For pertinent parameters see Table I.

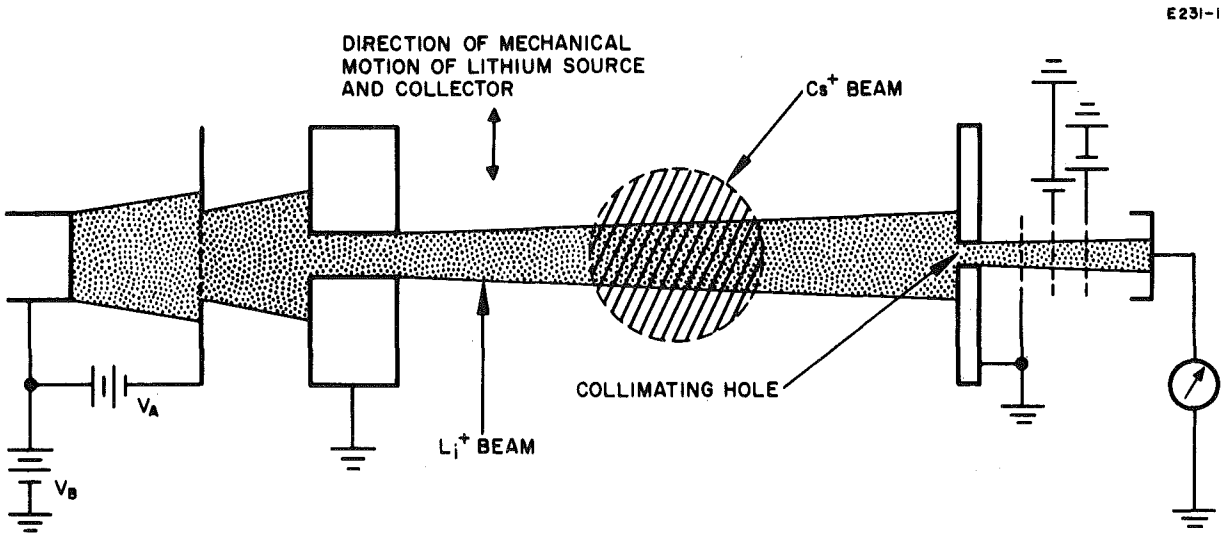

(a) Diagram of lithium beam probe for measurement of cesium beam potential.

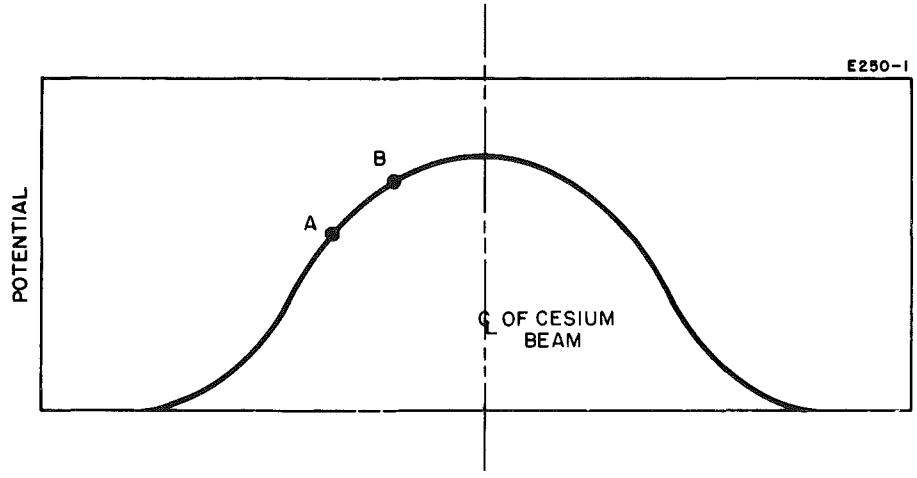

(b) Hypothetical beam potential of a cross section of the ion beam. Points A and B represent the boundary of the portion of the lithium beam which reaches the collector.

Fig. 9.

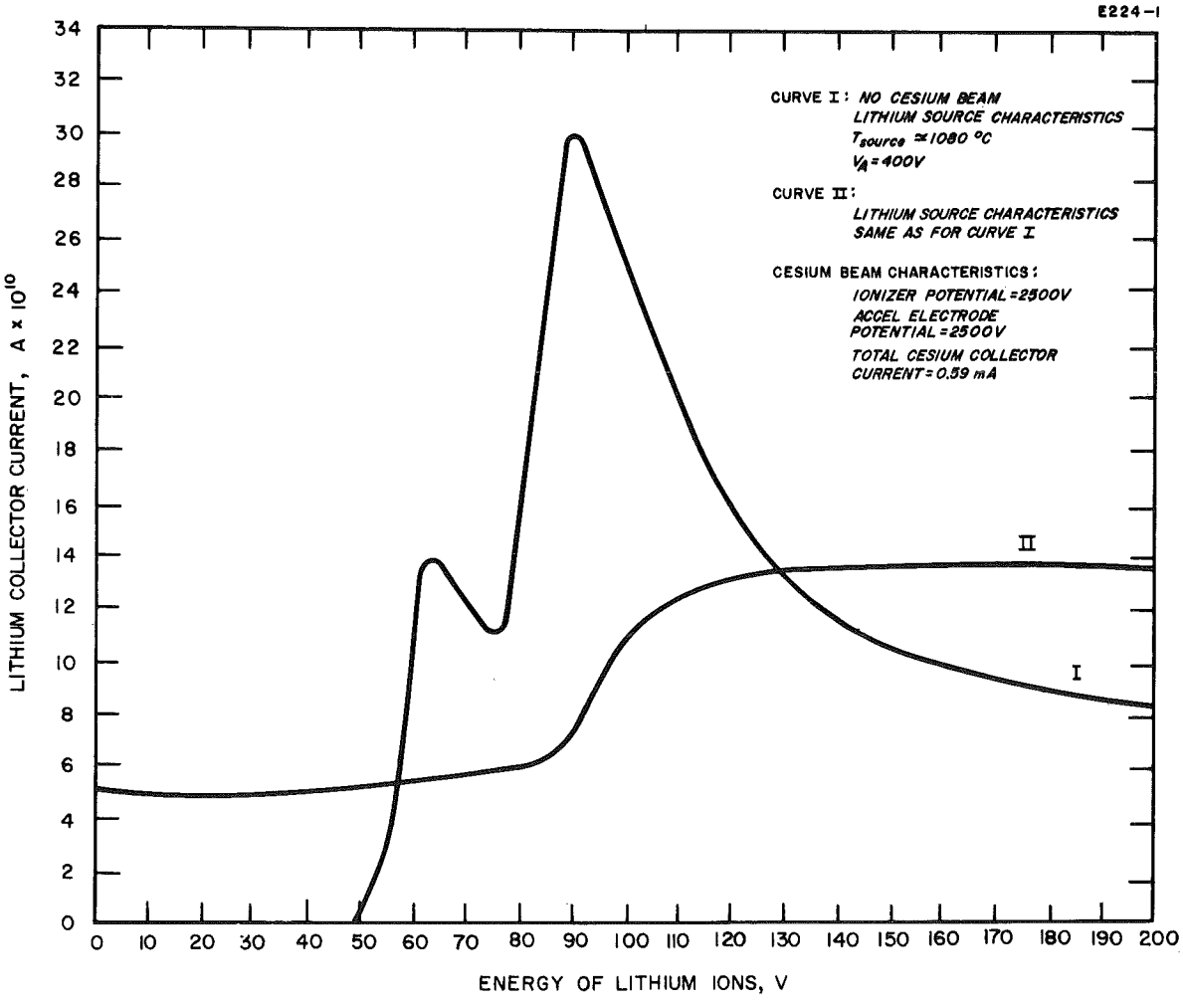

Fig. 10. Lithium collector response with and without cesium ion beam.

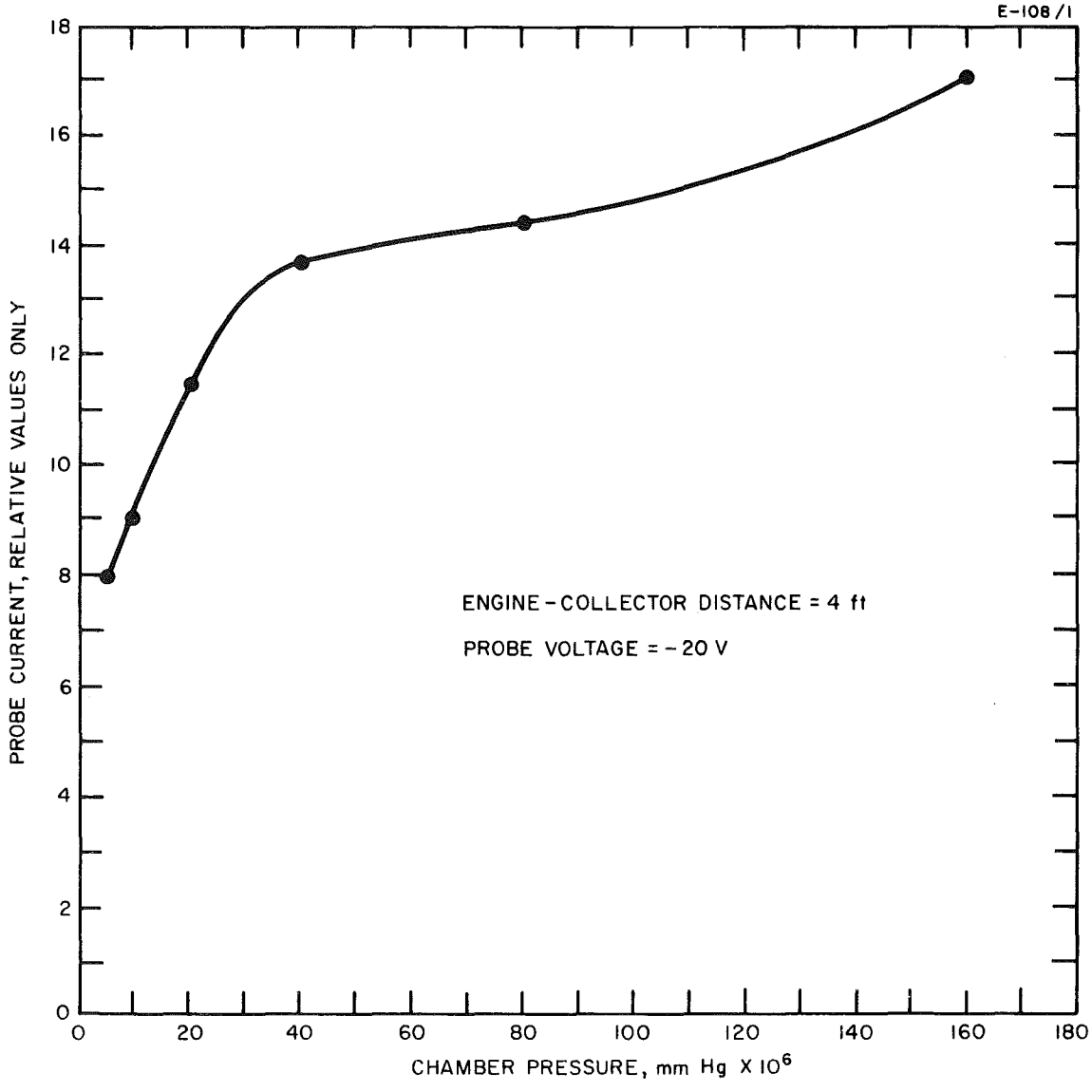

Fig. 11. Maximum window probe current versus chamber pressure.

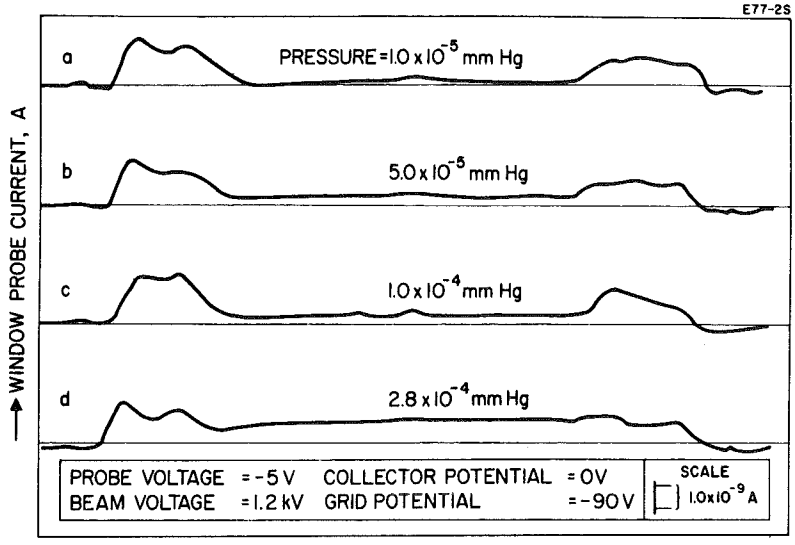

Fig. 12. Profiles of slow ion concentration in the annular ion beam with the window probe facing away from the engine.

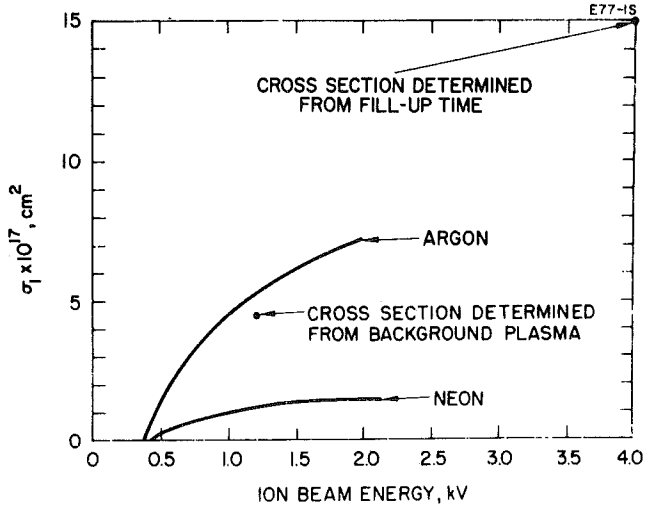

Fig. 13. Cross section for ionization by cesium ions of argon and neon (Ref. 5) and of air (these experiments.

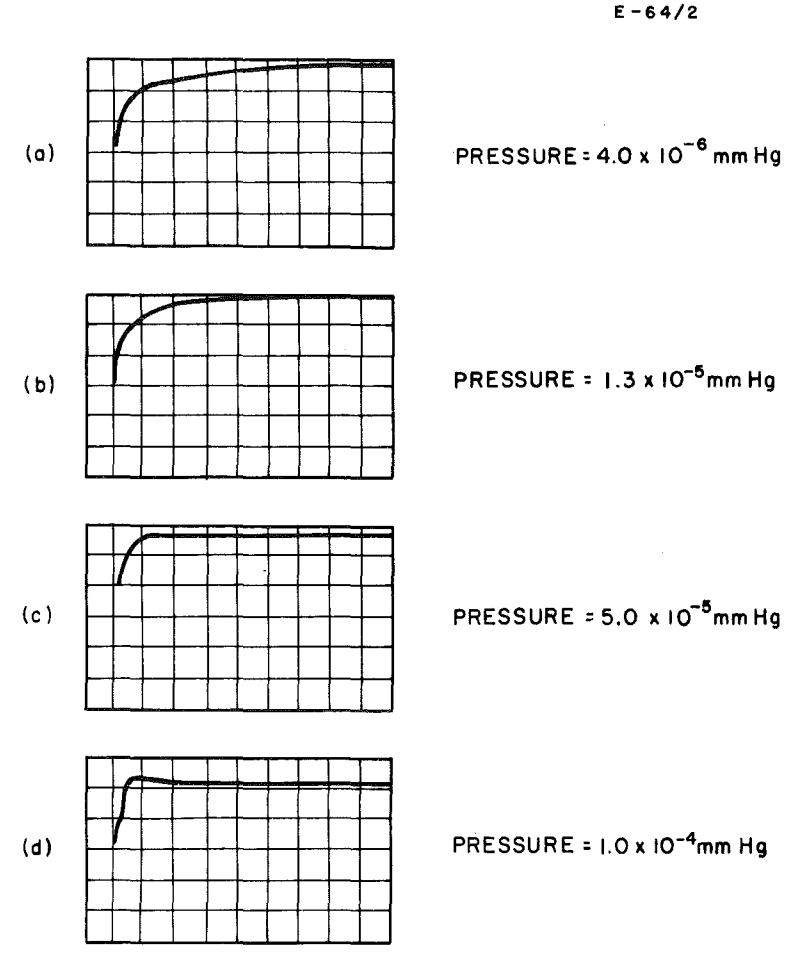

Fig. 14. Effect of pressure on fill-up time.

Collector distance = 10 ft.
Collector potential = 90V
Pulse length = 5 μsec
Pulse amplitude = 600 V
Scope setting:
collector current = 2 mA/div
time scale = 0.5 msec/div

REFERENCES

1. J. M. Sellen and R. F. Kemp, "Cesium ion beam neutralization in vehicular simulation," ARS Preprint No. 61-84-1778 (1961).

2. J. W. Ward and R. A. Hubach, "Neutralization of ion beams from engines of annular geometry," ARS Journal 32, 1730 (1962).

3. G. R. Haste and C. F. Barnett, "Plasma potential measurements using an ion beam probe," J. Appl. Phys. 33, 1397 (1962).

4. R. A. Hubach, "Probe for the measurement of albedo electron flux in a high-energy ion beam," Rev. Sci. Instr. 33, 1353 (1962).

5. J. C. Mouzon, "The ionization of noble gases by positive alkali ions — a correction," Phys. Rev. 44, 688 (1933).

6. G. J. Schulz and S. C. Brown, "Microwave study of positive ion collection by probes," Phys. Rev. 98, 1642 (1955).

7. R. C. Speiser and R. H. Vernon, ARS Preprint No. 2068-61 (1961).

8. J. C. Mouzon, "The ionization of neon and argon by positive alkali ions of energies from 650 to 2000 volts," Phys. Rev. 41, 605 (1932).

9. R. Bernas, L. Kaluszyner, and J. Druaux, "Sur la neutralization de la charge d'espace des faisceaux d'ions positifs par accumulation d'electrons; étude du temps de neutralization," J. Phys. Radium 15, 273 (1954).

APPENDIX – LITHIUM GUN COLLECTOR RESPONSE

The shape of the current-voltage curve of the lithium gun can be explained by considering two effects. The first is the effect of thermal velocities at low longitudinal velocities, and the second is the lens effect of the accel-decel system.

The lens system works as shown in Figs. A-1 and A-2. For the anode lens

$$\frac{V_A}{V_B} = 1.0$$

$$f = \frac{r_o}{r'} = \frac{0.1 \times \frac{0.060}{\pi}}{0.029} = 0.066 \text{ in.}$$

where r_o is the distance of the particular ion from the center line as it passes the first grid, and r' is the rate at which it diverges from the center line. For the aperture-cylinder lens*

$$\frac{V_A}{V_B} = 10$$

$$f_1 = 0.5 \times D_1 = 0.5 \times 0.125 = 0.063 \text{ in.}$$

The focal length of the aperture-cylinder lens does not change appreciably with further increase of voltage ratio. This indicates that the maximum transmitted current from focusing considerations should occur at $V_2/V_1 \approx 10$. Consideration of this lens effect leads to a current-voltage characteristic such as that shown in Fig. A-3.

The following analysis shows that thermal velocities also can affect the current voltage characteristic of the lithium gun. Assume that the average transverse velocity is entirely determined by kT and that the temperature is 1400°K.

*K. R. Spangenberg, Vacuum Tubes (McGraw-Hill, New York, 1948), p. 343, Fig. 13.34.

$$kT = 1.38 \times 10^{-23} \times 1400 = 1.93 \times 10^{-20}$$

$$= 0.12 \text{ eV}.$$

If we consider a point source emitting from the bottom of a cylinder, we find that the collector current for a given beam voltage is inversely proportional to the thermal energy.

$$I_{coll} \sim \frac{1}{\left(\frac{v_T}{v_Z}\right)^2} = \frac{V_B}{0.12}$$

This also shows that at low values of V_B the current measured at the collector should be directly proportional to V_B (from thermal velocity considerations alone), as demonstrated in Fig. A-4.

When these two effects are considered simultaneously, a current-voltage characteristic such as that of Fig. A-5 may result. This is precisely the type of response which is most generally observed, and consequently the proposed explanation may be correct.

To make this a more constant current (with respect to V_B) source it is proposed to make the drift space within the gun, between grids two and three, longer and narrower. This modification is being made in the new gun being designed for the small glass system.

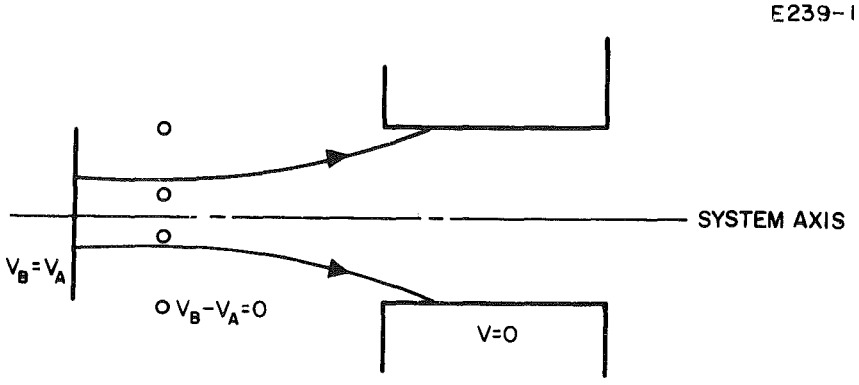

Fig. A-1. Lens effect at potentials noted.

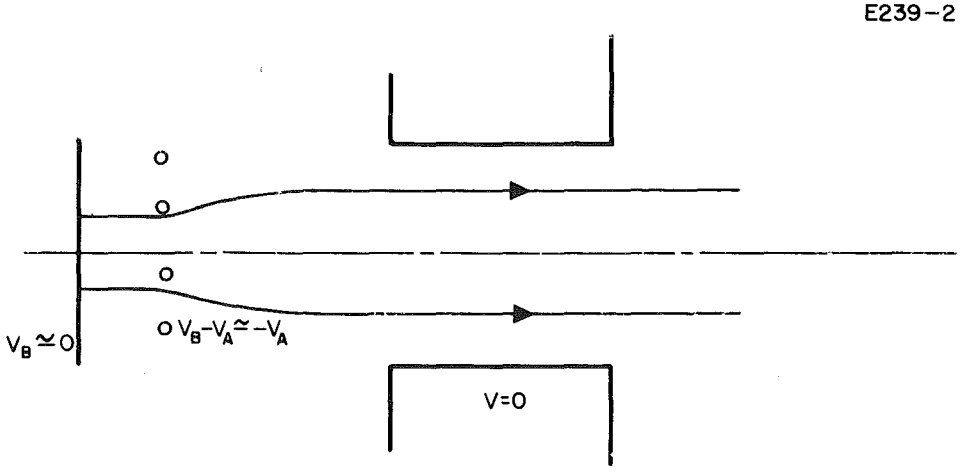

Fig. A-2. Lens effect at potentials noted.

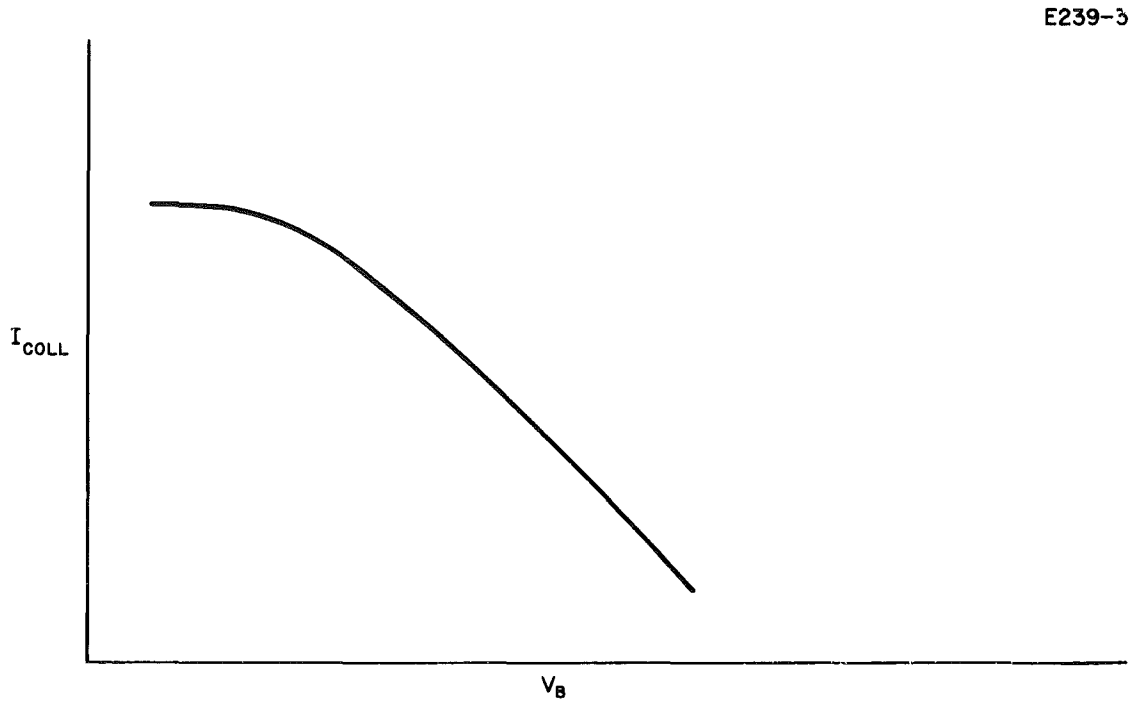

Fig. A-3. Current characteristics due to the lens effect.

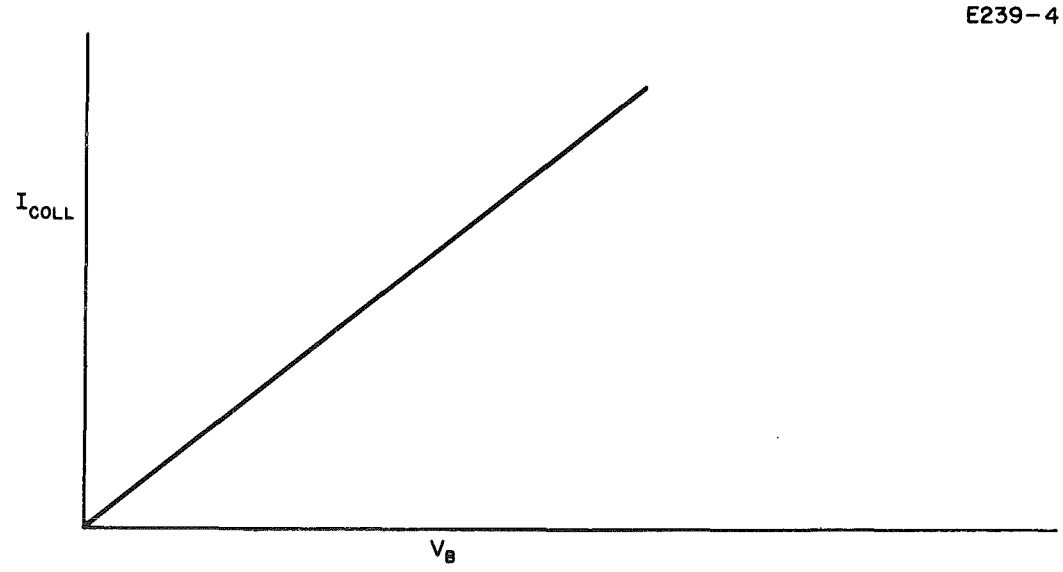

Fig. A-4. Current characteristic due to thermal velocities.

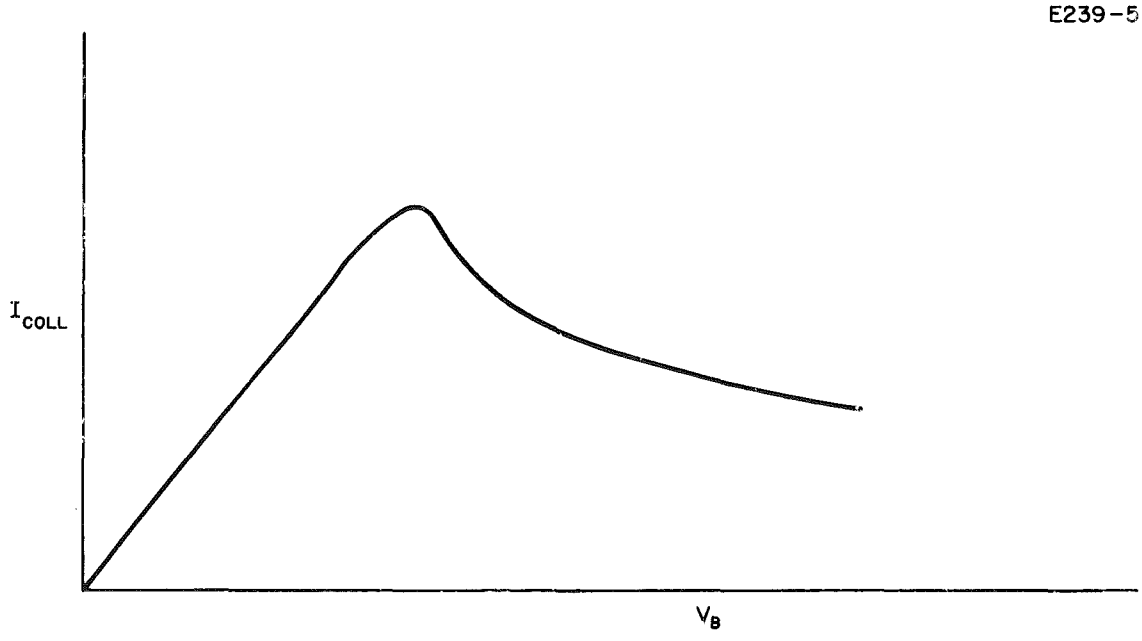

Fig. A-5. Superposition of the effects displayed in Figs. A-3 and A-4.

LIST OF SYMBOLS

A_w	area of aperture of window probe
f	ratio of r_o to r'
i_1	measured current through the fixed resistance in the isolated engine experiment (IEE)
i_2	leakage current in IEE
I_{coll}	lithium collector current
I_w	current through the aperture of the window probe
J	high energy cesium ion current density
L	a characteristic dimension of the ion beam
M	mass of positive ion
n_B	random plasma density
n_o	neutral cesium density
N_o	density of particles of the residual gas in the vacuum
r'	rate at which the ion diverges from the axis of symmetry
r_o	distance of a particular ion from the axis of symmetry of the lithium gun
R_s	shunt or leakage resistance between engine and ground in IEE
t_c	charging time in EDD
t_d	discharge time in IEE
T_-	electron temperature
v	velocity of slow ions, velocity of ions in cesium beam
v_T	transverse velocity of a lithium ion
v_Z	axial velocity of a lithium ion
V_A	potential between lithium ion source and the first grid

LIST OF SYMBOLS (cont'd)

V_B	energy of the beam of lithium ions in volts
V_E	potential placed between the exit electrode and electron emitter in IEE
V_M	maximum potential in the cesium beam encountered by the lithium beam
V_N	electron emitter heater voltage
V_o	minimum potential reached during discharge cycle in IEE
V_1	maximum potential reached during charge cycle in IEE
σ_{EX}	cross section for charge exchange
σ_I	cross section for gas ionization
τ_1	length of time an ion created by gas ionization lingers within the beam
cw	continuous wave = dc